

Thermal quenching of electronic shells and channel competition in cluster fission

Constantine Yannouleas and Uzi Landman

School of Physics, Georgia Institute of Technology, Atlanta, Georgia 30332-0430, USA

C. Bréchnignac, Ph. Cahuzac, B. Concina, and J. Leygnier

Laboratoire Aimé Cotton, CNRS Bât. 505, Campus Orsay, 91405 Orsay cedex, France

(April 2002)

Experimental and theoretical studies of fission of doubly-charged Li, Na, and K clusters in the low fissility regime reveal the strong influence of electronic shell effects on the fission products. The electronic entropy controls the quenching of the shell effects and the competition between magic-fragment channels, leading to a transition from favored channels of higher mass symmetry to the asymmetric channel involving the trimer cation at elevated temperatures.

Pacs Numbers: 36.40.Wa, 36.40.Qv, 36.40.Cg

Explorations of factors controlling the stability of finite systems, and of the collapse or fragmentation processes that may ensue when materials' stability boundaries are crossed, have served for a long time as sources of discovery in various areas of fundamental and technological research. These investigations range from early studies of hydrodynamical instabilities and droplet formation [1] to studies of fission and fragmentation in atomic nuclei [2], and of atomic and molecular free clusters and supported nanostructures [3,4]. Here we focus on fission of doubly charged cationic metal clusters caused by charge instabilities that develop subsequent to double ionization, that is $M_N^{2+} \rightarrow M_P^+ + M_{N-P}^+$. Such instabilities in macroscopic fluid systems have been studied by Rayleigh [1], and adaptations of Rayleigh's model (RM) for the description and analysis of nuclear [2] and cluster fission [5] are referred to as the Liquid Drop Model (LDM). When the LDM is combined with the jellium-background picture, the clusters are viewed as charged classical liquid drops whose shape and dynamics are controlled by the competition between the repulsive Coulomb (E_{Coulomb}) and the binding surface (E_{surface}) energies [6].

An important result of the RM concerns the critical size $N_{\text{cr}}^{\text{RM}}$ below which the clusters are unstable against barrierless fission. The pertinent parameter is the fissility $X = E_{\text{Coulomb}}^{\text{sph}}/2E_{\text{surface}}^{\text{sph}}$, where the superscript "sph" indicates that the equilibrium shapes of the LDM are spherical. For $X \geq 1$, spontaneous barrierless fission is predicted and observed [7,8]; this is also the regime studied originally by Rayleigh who predicted a mass-symmetric fission mode (see also Ref. [7]). In the $X < 1$ regime, which is the focus of our paper, the fissioning system must overcome a barrier. For nuclei, spontaneous sub-barrier fission via tunneling can still occur for $X < 1$,

while for atomic clusters, tunneling is suppressed and fission in this regime requires thermal activation. From the relation $X_{\text{cr}} = 1$, the barrierless RM critical size is $N_{\text{cr}}^{\text{RM}} = z^2 e^2 / (16\pi r_s^3 \sigma)$, where r_s is the Wigner-Seitz radius and σ is the surface-energy; for doubly charged ($z = 2$) Li, Na, and K clusters, one has $N_{\text{cr}}^{\text{RM}} \approx 10$. As a result, with the exception of the smallest ones, fissioning clusters must be hot in order to overcome the fission barrier. At finite temperature, the fission processes compete with other decay channels, e.g., evaporation of neutral monomers and dimers [see Eq. (1b)]. While this was recognized early on [9], a systematic understanding of thermal effects in fission is still lacking.

Another principal result of the LDM pertains specifically to the low fissility $X < 1$ regime. Based on the Q^T -values for finite temperature [6,10], $Q_P^T = F_P^+ + F_{N-P}^+ - F_N^{2+}$, that express the free-energy balance for the possible ($P, N - P$) fission channels, the LDM predicts the dominance of a strongly mass asymmetric fission process. Such asymmetric fission has been observed in experiments for Na_N^{2+} with $N \sim 24$ (i.e., near the appearance size, see below), where it was found that the preferred fission channel involved the "magic" Na_3^+ fragment [9]. The prevalence of this channel, compared to other asymmetric ones in the neighborhood of the LDM minimum, originates from quantum mechanical shell effects [11].

In this paper we present experimental and theoretical results, pertaining to trends in the cluster fission channels for $X \ll 1$, which unquestionably cannot be accounted for within the classical framework of the RM. Instead we demonstrate the dominance of quantum-size effects, i.e., electronic shell contributions [6]. In particular, we study here the larger sizes ($N = 24, 26, 28$, and 30) of clusters of the alkali metals Li, Na, and K. These larger systems correspond to the lowest observable fissility regime with $N \gg N_{\text{cr}}^{\text{RM}}$; e.g., for $N = 30$ one has $X \approx 0.25$ for the doubly charged alkali clusters. Moreover, this range of sizes is particularly suitable for explorations of shell effects, since it includes cases where the clusters may fission into doubly "magic" fragments, i.e., $M_{24}^{2+} \rightarrow M_{21}^+ + M_3^+$ and $M_{30}^{2+} \rightarrow M_{21}^+ + M_9^+$.

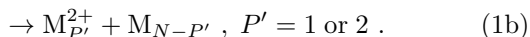
We find that in addition to M_3^+ the more mass symmetric magic fission channels (M_9^+ and M_{21}^+) do appear and compete with the channel involving the trimer, even becoming the preferred channels in several instances. Furthermore, from comparisons between the experiment

and calculations based on the finite-temperature shell-correction method (FT-SCM) [12], we find that the channel distributions are greatly influenced by thermal quenching of the shell effects due to the increase (compared to $T = 0$) of the electronic entropy; this quenching results from thermal promotion of electrons to unoccupied single-particle levels which smears out the shell structure. The more mass-symmetric fission channels are favored at lower temperatures, whereas the asymmetric ones (e.g., involving the M_3^+ fragment) dominate as T increases. These trends reflect the more pronounced (quenching) effect of the electronic entropy on the shell-stabilization of the larger magic sizes (e.g., M_9^+ and M_{21}^+).

The experiment [13] consists of a distribution of relatively large neutral clusters formed by a gas aggregation source. The clusters are ionized, photo-excited and warmed by a 15 ns laser pulse (Nd-YAG laser at $h\nu = 3.50$ eV). A rapid sequential evaporation follows the warming of the clusters during about $1 \mu\text{s}$, which is the residence time of the clusters in the ionizing region. This results in a charged cluster distribution shifted down to smaller sizes, called an “evaporative ensemble” [13] of clusters. It has been demonstrated that the cluster temperature associated with the evaporative ensemble is determined by the cluster dissociation energy and by the experimental time window, i.e., the residence time in the ionizing/heating region [13]. Under our experimental conditions the temperatures of the evaporative ensembles of lithium, sodium and potassium clusters are 700 ± 100 K, 400 ± 100 K and 300 ± 100 K, respectively.

The evaporative ensemble of ionized clusters enters a tandem time-of-flight (TOF) mass spectrometer. Parents of interest are mass selected in the first TOF region. Because they are at a given temperature, subsequent unimolecular dissociation of these parents takes place and the resulting fragments are mass analyzed by the second TOF device. Improvements made by us over our previous experiments (via optimization of the electrostatic potentials) lead to significant increases in both the mass and energy resolutions. In particular, the latter allows us to resolve the kinetic energy released during the fission process (see the splitting of the peak of some of the fission fragments in Fig. 1).

For cluster sizes in the vicinity of the appearance size (see below), the unimolecular dissociation of doubly charged clusters portrays the competition between the fission (1a) and evaporation (1b) processes:



We focus here on the fission decay channels. The explored size domain is bounded by two values, N_- and N_+ . The lower value N_- is determined by the appearance size N^{app} ($N^{\text{app}} = 24$ for Li_N^{2+} and Na_N^{2+} clusters, and 19 for K_N^{2+} clusters [4]), below which fission is the

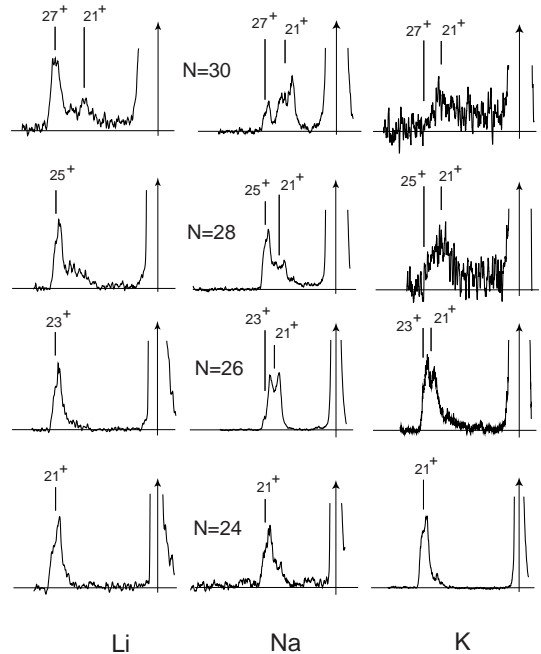


FIG. 1. Fission channels recorded in TOF measurements for Li_N^{2+} , Na_N^{2+} , and K_N^{2+} clusters, with $N = 24, 26, 28$, and 30 . In each case, the peak on the right (marked by an arrow) corresponds to the parent cluster and the ones on the left of it correspond to the larger fission fragments. Fragment labelings are determined from the voltage setup. Peak heights are in arbitrary units. The splitting of the TOF ion-fragment peaks are due to the kinetic energy released during fission, which is of the order of 1 eV (see, e.g., the case $N = 26$).

dominant dissociation process [see Eq. (1a)]. Below this size no doubly charged clusters are present in the mass spectra, since their fast fission process prevents their observation during the experimental time window. N_+ is determined by the loss of the signal corresponding to the fission process, resulting from the increase of the inner part of the fission barrier with the size of the cluster relative to the essentially constant monomer evaporation energy. Fig. 1 summarizes the results obtained for the three alkali metals in the same size range. The improvement of the experimental sensitivity and the energy resolution over our previous studies allowed us to extend the observation of fission to $N = 30$, i.e., well above both the RM critical stability and the appearance sizes.

Although we have recorded the fragmentation spectra for all the sizes $24 \leq N \leq 30$, only results for clusters with an even number of atoms are shown, since due to pairing effects they exhibit simpler features. In our experimental setup, only the heavy fragments M_P^+ with $P > N/2$ are detected. The main features are as follows: For the lowest parent size ($N = 24$) and for all three elements, only one fission channel is present, i.e., the doubly magic $M_3^+ + M_{21}^+$. Increasing the parent size, however, results in differentiation between the three elements re-

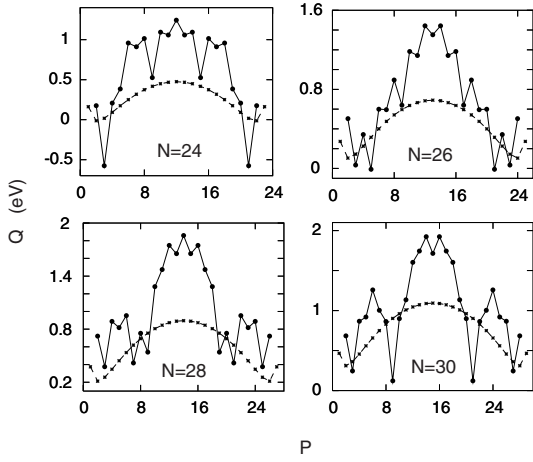


FIG. 2. Theoretical SCM zero-temperature energetics (Q -values) for the processes $\text{Li}_N^{2+} \rightarrow \text{Li}_P^+ + \text{Li}_{N-P}^+$, $N = 24, 26, 28,$ and 30 . The dashed lines correspond to LDM calculations. In each case, the horizontal axis corresponds to various channels $2 \leq P \leq N - 2$.

garding the observed fission channels. A larger parent size (i.e., $N \geq 26$) opens the channels of heavier fragments and this trend is more pronounced for potassium than for lithium. In particular, the trimer appears to be the dominant product in the lithium fission, while M_{21}^+ is the dominant one in the potassium fission, with sodium exhibiting an intermediate behavior. In other words, the asymmetry of the fission process is reduced for the potassium clusters as compared to the sodium and to lithium ones.

To elucidate these experimental observations, we have performed FT-SCM calculations of the Q^T -values for the various fission channels for all three alkali-metal sequences at the corresponding experimentally determined temperatures. Since for each species the Coulomb repulsion at the scission point (measured by the energy release) is approximately constant for all fission channels in the size-range considered here ($X \ll 1$), the effective inner part of the fission barrier can be approximated by adding the calculated Q^T -values to it. Thus the ordering of the fission channels can be directly inferred from the Q^T -values.

As we elaborate below, the theoretical zero-temperature Q -values provide an inadequate description of the experimental data. For example, the Q -values for Li_N^{2+} (plotted in Fig. 2) cannot explain the observed trend (see Fig. 1, left column) of strong asymmetric fission, with the Li_3^+ being the preferred channel for all parents $N = 24, 26, 28,$ and 30 [14]. In particular, the $T = 0$ theoretically deduced preferred fission channels for $N = 26$ and $N = 30$ are (5,21) and (9,21), respectively, in contradiction with the measurements (see Fig. 1). In contrast, the theoretical Q^T -values presented in Fig. 3 are in excellent agreement with the experiment. In particular, for

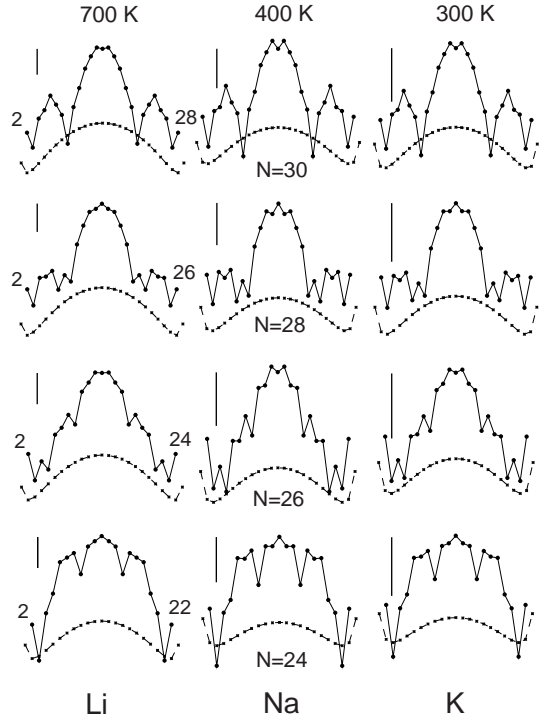


FIG. 3. Finite-temperature SCM results (Q^T -values) for the fission process $\text{M}_N^{2+} \rightarrow \text{M}_P^+ + \text{M}_{N-P}^+$ for Li_N^{2+} , Na_N^{2+} , and K_N^{2+} with $N = 24, 26, 28,$ and 30 . The corresponding temperatures (in degrees Kelvin), taken from the experiments, for each species are shown at the top. The dashed lines correspond to LDM calculations. In each case, the horizontal axis corresponds to various channels $2 \leq P \leq N - 2$. The length of the vertical bar in each frame corresponds to 0.4 eV.

Lithium the theoretical results at $T = 700$ K show that Li_3^+ is indeed the preferred channel for all parents; only for Li_{30}^{2+} , the Li_{21}^+ channel becomes a competing one, remaining however less abundant than the one involving the trimer.

We stress again that in Fig. 3 there is a clear tendency toward opening the channels involving the heavier magic fragments ($P = 9$ and $P = 21$), both when going up vertically from the lighter to the heavier parents (from $N = 24$ to $N = 30$), as well as when going horizontally from left to right (i.e., from Li to K, with Na representing an intermediate case).

The physics underlying this agreement between the experiment and the FT-SCM results can be revealed by an examination of the influence of the electronic entropy on the various fission channels ($P, N - P$) as a function of P . For brevity, we limit our discussion to the case of the K_{30}^{2+} parent; the conclusions, however, extend to all three species and the other parent sizes. Figure 4 displays the FT-SCM Q^T -values for K_{30}^{2+} at five temperatures, starting with $T = 200$ K and increasing to $T = 1000$ K. At the lowest temperature, the (9, 21) channel is the preferred one; however, we observe that an increase in T is accom-

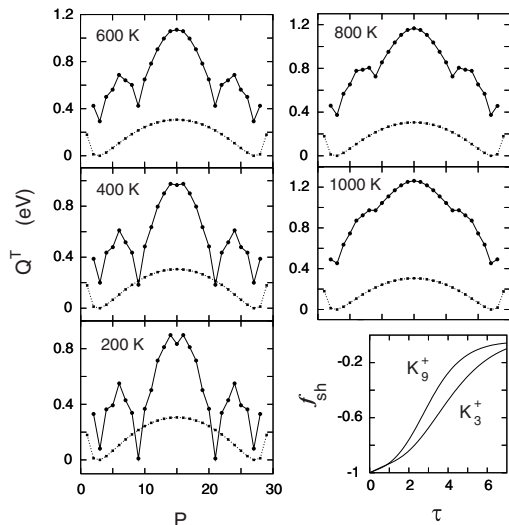


FIG. 4. Theoretical FT-SCM temperature dependence of the Q^T -values for the process $K_{30}^{2+} \rightarrow K_P^+ + K_{30-P}^+$. The dashed lines correspond to LDM calculations. In each case, the horizontal axis corresponds to various channels $2 \leq P \leq N - 2$. In the bottom right frame, we display f_{sh} vs. τ (see text) for the K_3^+ and K_9^+ fragments.

panied by a quenching of the shell effects; i.e., at high temperature (1000 K) the shell effects have almost vanished, and the Q^T -value curve exhibits a smooth shape similar to that of the LDM (although with a steeper variation).

Most important for the competition between the various magic fragments, however, is the fact that the electronic-entropy quenching of the shell effects is non-uniform, with the higher occupied shells of the heavier fragments being influenced first as T increases, since the energy spacing, $\hbar\omega_0(N) = 49 \text{ eV} \cdot a_0^2 / (r_s^2 N^{1/3})$, between the major electronic shells decreases with a larger N . Consequently, a higher T favors the trimer (M_3^+) channel over those involving the magic M_9^+ and M_{21}^+ fragments. This happens even in the case of $N = 30$ where the competing (9, 21) channel is doubly magic. Note that, unlike the $T = 700 \text{ K}$ experimental temperature of Li, the temperatures of 300 K for Potassium and 400 K for Sodium are low enough so that the heavier-fragment channels retain their $T = 0$ original prevalence for all three parent sizes $N = 26, 28, \text{ and } 30$.

Further insight can be gained by examining the ratio $f_{\text{sh}}(N) \equiv \Delta F_{\text{sh}}(N, \tau) / |\Delta F_{\text{sh}}(N, 0)|$ of the free-energy shell-correction term at $\tau = 2\pi^2 kT / \hbar\omega_0(N)$ over the shell correction term at $\tau = 0$. For a schematic single-particle spectrum consisting of equally spaced degenerate shells with the same degeneracy, it can be shown [2,10] that $f_{\text{sh}}(N) \approx -\tau \exp(-\tau)$ for $\tau \geq 1$. Thus, because of the factor $2\pi^2$, the electronic-entropy effects may be expected to manifest themselves even at the rather low temperatures of the cluster experiments. In Fig. 4 (bottom frame

on the right), we compare f_{sh} for K_9^+ and K_3^+ calculated for the realistic single-particle spectrum of our FT-SCM. It is seen that the realistic spectrum tends as a function of T to suppress the shell effect of the magic fragments that are heavier than the trimer at a rate which is faster than the estimate given above.

The controlling influence of the electronic entropy on the stabilization of electronic shells, discussed previously [6,10] in studies of ground-state properties of clusters, has been found here to govern the fission patterns and their temperature dependence at the low-fissility regime. The agreement obtained between the improved experiments and the temperature-dependent shell-correction calculations provides insights into the factors governing the competition between fission channels and points to the need for further temperature-controlled studies of charge instabilities in clusters.

This research is supported by the US D.O.E. (Grant No. FG05-86ER-45234).

-
- [1] L. Rayleigh, *Phil. Mag.* **14**, 184 (1882).
 - [2] Å. Bohr and B.R. Mottelson, *Nuclear Structure* (Benjamin, Reading, 1975) Vol. II.
 - [3] U. Landman *et al.*, in *The Physics and Chemistry of Clusters*, Proc. Nobel Symposium **117**, edited by E.E.B. Campbell and M. Larsson (World Scientific, Singapore, 2001), p. 42.
 - [4] C. Bréchnignac, in Ref. [3], p. 278.
 - [5] W. Saunders, *Phys. Rev. A* **46**, 7028 (1992).
 - [6] C. Yannouleas, U. Landman, and R.N. Barnett, in *Metal Clusters*, Edited by W. Ekardt (Wiley, Chichester, 1999), p. 145.
 - [7] C. Bréchnignac *et al.*, *Phys. Rev. Lett.* **72**, 1636 (1994).
 - [8] V.F. Chandezon *et al.*, *Phys. Rev. Lett.* **87**, 153402 (2001).
 - [9] C. Bréchnignac, Ph. Cahuzac, F. Carlier, and M. de Frutos, *Phys. Rev. Lett.* **64**, 2893 (1990).
 - [10] C. Yannouleas and U. Landman, *Phys. Rev. Lett.* **78**, 1424 (1997).
 - [11] R.N. Barnett, U. Landman, and G. Rajagopal, *Phys. Rev. Lett.* **67**, 3058 (1991).
 - [12] The FT-SCM [10] is an extension of the zero-temperature SCM [C. Yannouleas and U. Landman, *Phys. Rev. B* **51**, 1902 (1995); *ibid.* **48**, 8376 (1993)] and it incorporates three important elements, i.e., triaxial deformations, single-particle electronic entropy, and thermal averaging over the shape fluctuations. The SCM approach is based on the fact that the total free energy of a finite system of interacting delocalized electrons can be divided into two contributions, i.e., a part that varies smoothly with the system size and thus coincides with the LDM, and an oscillatory term accounting for the quantal shell effects. In keeping with the experimental analysis [13], the LDM curvature coefficients were taken to be zero, while

the surface coefficients for Li, Na, and K were taken as 1.30 eV, 0.85 eV, and 0.70 eV, respectively. The temperature dependence of these coefficients was neglected. For the rest of coefficients of the FT-SCM, see the first reference in this footnote for Na and K, and C. Yannouleas and U. Landman, *J. Chem. Phys.* **107**, 1032 (1997) for Li.

- [13] For details of the experimental apparatus, see C. Bréchnac, H. Busch, Ph. Cahuzac, and J. Leygnier, *J. Chem. Phys.* **101**, 6992 (1994).
- [14] Previous experimentally determined Q -values, obtained via Born-Haber cycles and employing a low-temperature value of the dimer dissociation energy, are in agreement with the theoretical zero-temperature SCM results.